ISSN 8755-6839

SCIENCE OF **TSUNAMI HAZARDS**

Journal of Tsunami Society International

**Volume 39** **Number 2** **2020**

# INDONESIAN TSUNAMI EARLY WARNING SYSTEM AUGMENTATION USING GNSS-TEC

**Buldan Muslim[1)] , Mokhamad Nur Cahyadi[2)], and Charisma Juni Kumalasari[3)]**

[1] *National Institute of Aeronautics and Space (LAPAN), Bandung 40173, Indonesia*

[2]*Department of Geomatics Engineering, Institut Teknologi Sepuluh Nopember Kampus ITS Sukolilo ,Surabaya, 60111, Indonesia*

[3]*Mathematics Department, Master's Programme, Institut Teknologi Sepuluh Nopember, Surabaya 60111, Indonesia*

*Corresponding author: mbuldan@gmail.com*

## ABSTRACT

The Indonesian tsunami early warning system (INATEWS) has been developed and operated after the tsunami struck Aceh in December 2004. The INATEWS is based on a relationship model of earthquake parameters and tsunami potential. At the tsunami observation stage, INATEWS is still experiencing difficulties due to limited buoy stations. Alternative tsunami observations have been investigated using ionospheric TEC data from

GPS signal observations. This paper reviews the methods that have been studied and used for tsunami detection using ionospheric total electron content (TEC) from GNSS data. Status and development plans of real-time GNSS resource utilization for TEC measurement in Indonesia and its application for INATEWS augmentation are also discussed.

**Keywords**: INATEWS, Total Electron Content (TEC), GNSS

## 1. INTRODUCTION

The Tsunami Early Warning System is designed to detect the emergence of tsunami and provide warning to prevent casualties. New concepts and procedures for the fast and reliable determination of strong earthquakes, the modeling and simulation of tsunami, and the assessment of the situation have been implemented in the warning system. To anticipate the earthquake (EQ) and tsunami hazard, in November 2008 a tsunami early warning system in Indonesia was launched, known as InaTEWS (Indonesian Tsunami Early Warning System). Earthquake data that are integrated with various data of early warning devices such as GPS buoys, and tide gauges will confirm whether tsunami waves have already formed or not. This information will be forwarded to the public. The Early Warning System is operated by BMKG. Information from the different sensor systems are processed in the Tsunami Early cancellations respectively. The experiences from the capacity development program for local communities have been made available in the form of the Tsunami Kit that provides practical concepts that have been tested and validated, materials and tools for ongoing and future initiatives to strengthen local warning chains and tsunami preparedness throughout Indonesia. It is important to keep in mind that the effectiveness of InaTEWS greatly depends on the ongoing and future efforts to develop the required capacities in the downstream process (Hanka et al. 2010).

Recent developments in Real-time Precise Point Positioning (RTPPP) GPS processing (Ge et al., 2011) made it possible to use co-seismic displacement vectors registered by GPS more efficiently in the early warning process especially in the case of near-field tsunami. Babeyko and co-workers presented their recent results using a limited number of Japanese GPS stations for the direct inversion of co-seismic displacements into the slip distribution of the 2011 Tohoku Earthquake (Babeyko and Hoechner, 2012). They demonstrated how the slip distribution of an earthquake can be calculated with sufficient accuracy for early warning purposes within 2-3 minutes with a sufficient number of GPS stations. These findings have also been confirmed by other groups (Wei et al. 2011). Together with near-real time Tsunami modeling tools, this result will open a new perspective to switch the early warning process especially for near-field cases from the static and database oriented approach using pre-calculated Tsunami scenarios to a forecast approach based on directly measured sensor information from seismic and GPS networks in real-time.

Indirect tsunami observations by measurements of radio wave propagation through the

ionosphere are based on ideas that have been anticipated in the past by Hines (Hines, 1972; 1974; Peltier and Hines,1976). Tsunami produces internal gravitational waves (IGWs) in an upward-spreading atmosphere. During upward propagation, IGWs are strongly amplified by atmospheric amplitudes due to the effect of decreasing atmospheric density to the extent of the atmospheric layer it passes. IGW interaction with plasma at ionosphere elevation in the results the variation velocity and density of plasma that can be observed by radio wave propagation in the ionosphere. Exciting research results on detection of the tsunamigenic peruvian earthquake on June 23, 2001 (M = 8.4 at 20:33 UT) to the total electron content (TEC) in ionosphere (Artru et al. 2005) which was measured by Japan's solid GPS network, GEONET opened up a modern debate on the feasibility of tsunami detection by radio wave propagation in the ionosphere. The gigantic tsunami of Sumatra-Andaman (Mw = 9.3, 0:58:50 UT, December 26, 2004 (Lay T et al. 2005) in which the magnitude larger than the Peruvian Tsunami, provides remote sensing observations worldwide in the ionosphere and an opportunity to explore ionosphere tsunami detection with large data sets. In addition to the seismic waves detected by global seismic networks (Park et al. 2005) co-seismic displacement is measured by GPS (Vigny et al., 2005); sea surface variations were measured by altimetry (Smith et al. 2005); detection of magnetic anomalies (Iyemori et al, 2005; Balasis and Mandea, 2007) and acoustic gravity waves (Le Pichon et al. 2005); a series of ionospheric disorders has been reported in recent literature using different techniques, such as Doppler sounding (Liu et al. 2006), over-the-horizon radar (Occhipinti et al. 2006), GPS (Liu et al. 2006; Lognonné et al., 2006; DasGupta et al. 2006) and altimeter (Occhipinti at al. 2006). Most observations show the relationship of Rayleigh waves in the ionosphere and tsunami. Numerical modeling by considering coupling between the lithosphere / atmospheric / ocean / atmospheric-neutral / ionosphere (Occhipinti et al, 2006; Occhipinti et al, 2008; Mai and Kiang, 2009; Hickey et al, 2009) produced several observations that proved the relationship between ionosphere impairment and displacement surfaces generated by Rayleigh waves and tsunami (Occhipinti et al. 2006).Through recent progress in tsunami detection using radio wave propagation in the ionosphere, we reviewed the results of detection methods of TEC disturbance caused by tsunami caused by 2004 Sumatra Earthquake until the 2011 tsunami in Tohoku. In addition we discussed a potential GNSS data network in Indonesia that could potentially be used to strengthen tsunami early warning in Indonesia.

## 2. REVIEWS OF DETECTION METHODOLOGY OF TSUNAMI EFFECT ON THE IONOSPHERE FROM GNSS DATA

### 2.1 High pass filter

Arthru used a high pass filter with a cut-off at 30 minutes to remove diurnal variation and receiver bias (Artru et al. 2005). Using single satellite observation to reduce mislocation of ionospheric pierce points (IPP), where the relative location of the different measurement points is still accurate. The traveling ionospheric disturbances (TID) are the common phenomenon of during day and night. In order to confirm that the tsunami, the preceding

and following days are used as a reference. The criteria of wave-like perturbation of TID are more than 0.1 TECU. The daytime TID is more frequent than the nighttime TID.

### 2.2.2 Polynomial and band pass filtering

According to Galvan et al.(2011) used polynomial function to fit the TEC time series in order to fit the longer period variations such as diurnal variations and elevation angle dependence of the TEC ray path. After that they used a band pass filter of 0.5 - 5 mHz (corresponding to wave period of 33.3 to 3.3 minutes, a typical range of tsunami periods) to extract TID caused by tsunami.

### 2.3 Cut off TEC error: Three-sigma TEC error measurement (0.03 TECU)

The precision of GPS carrier phase measurement is less than 1 mm. According to the error propagation law, the measurement error of TEC is about 0.01 TECU. The detrended TEC in quiet condition is nearly the random noise, which is dominated by the measurement error. In quiet condition the detrended TEC value will usually fall into the three-sigma range of about 0.03–0.03 TECU. When the detrended TEC values are out of this range, the TEC anomalies could be detected. The high precision and high temporal-spatial resolution ionospheric TEC from GEONET provides the opportunity to discuss the detailed seismic ionospheric pattern and evolution (Jin et al. 2009).

### 2.4 Detrending STEC map with 10 minutes windows.

According to Tsugawa et al.(2011) used detrended TEC by subtracting TEC from 10 minutes windows moving average for detecting Tohoku tsunami effect on ionosphere using GEONET data.

### 2.5 Four-order zero phase shift Butterworth filter

According to Jin et al.(2014) corrected the times in GEONET by adding the difference between UTC and GPS time with 15 s on 11 March 2011 according to the International Earth Rotation and References Systems Service (IERS) Bulletins (http://hpiers.obspm.fr/eop-pc/). In order to degrade the multipath effects and the error of mapping function, measurements with low satellite elevation angles (less than 10° if not specified in following) are not used. In order to remove the TEC trend and high frequency fluctuations and other noises, the detrended TEC series are filtered with four-order zero phase shift Butterworth filter that is designed with a most flat frequency response in the pass band without phase shift. Here the TEC series obtained by GEONET dual frequencies GPS measurements are filtered with a 1–15 mHz window for detrending. The trend is mainly caused by SIP's motion and ionospheric background changes. They choose the 15 mHz as the high cut-off frequency in consideration of the 30 s interval of the GEONET ionospheric monitoring, avoiding the aliasing in signal processing and chose 1 mHz as a threshold to remove the background TEC variation. For Tohoku tsunami, TEC measurement near the epicenter could detected the acoustic wave and wave related to the Rayleigh wave (3–7 mHz) and tsunami-generated gravity wave (<3 mHz)

(Matsumura et al, 2014; Occhipinti et al, 2013) but also higher frequencies signal (7–15 mHz).

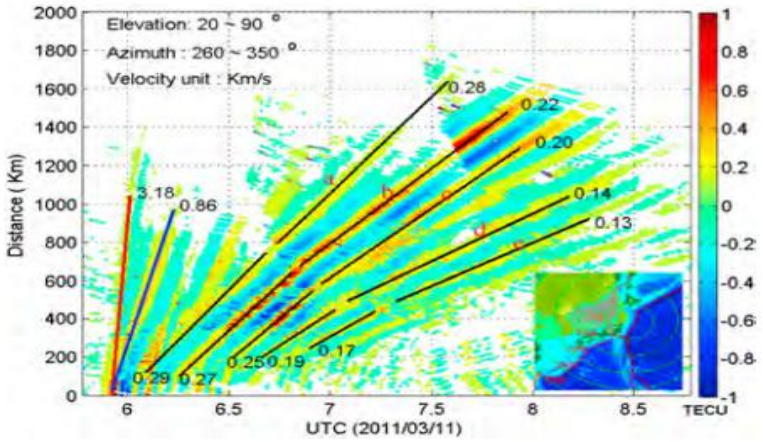


Figure 1. Travel time diagram of post-seismic TEC disturbances following the Tohoku earthquake on 11 March 2011. The SIP with azimuth angles of 260-350$^0$ and satellite elevation angles of 20-90$^o$ are used. The disturbance amplitude is described by the scale color. The bottom right figure shows the SIP location area with a yellow sector patch. The red circles are equidistant lines to the epicenter corresponding to 500-2500 kms with a 500 kms interval (Jin S et al. 2014).

Figure 2 presented TEC disturbance time series and spectrograms around the epicenter from 05:00 UTC to 09:00 UTC. Here, the one-sided normalized power spectral density (PSD) is computed using the short-time Fourier transform. The length of the window is set as 30 min. In the upper left panel, the star is the location of the epicenter, and the circle is the location of the corresponding GEONET station. The black line is SIP's.

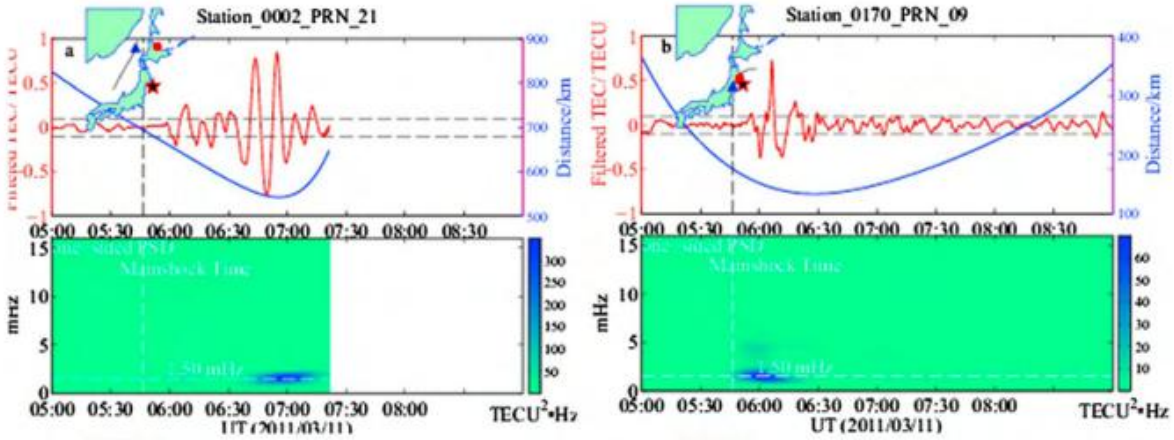


Figure 2. TEC disturbance time series and spectrograms around the epicenter from UTC 05:00 to UTC 09:00 (Jin S et al. 2014).

## 2.6 Adopted a simple ray-tracing technique commonly used in seismology

A simple ray-tracing technique (Aki and Richards, 2002) commonly used in seismology was employed here in to estimate the arrival times at the 12 monitoring stations for locating the earthquake source (or tsunami origin) as well as to find if the observed disturbances of the ionospheric GPS TEC is triggered by the tsunami. Firstly they try to guess a location of the tsunami source; calculate travel time of the tsunami propagating horizontally away from the trial source and triggering the acoustic gravity wave which in turn propagates vertically to reach each monitoring station; and compute a standard deviation of the differences between the calculated and the observed arrival times. They repeat this procedure through the whole set of grid points (trial source locations) and then contour the computed standard deviations to find the minimum, which is then considered to be a possible source.

Figure 3 shows that an average horizontal speed of 191 m/s (about 700 km/hr) and an average vertical speed of 730 m/s give an optimal induced time at 0106 UT±15 min and source location at – 1N, 93E which is about 580 km southwest of the earthquake epicenter.

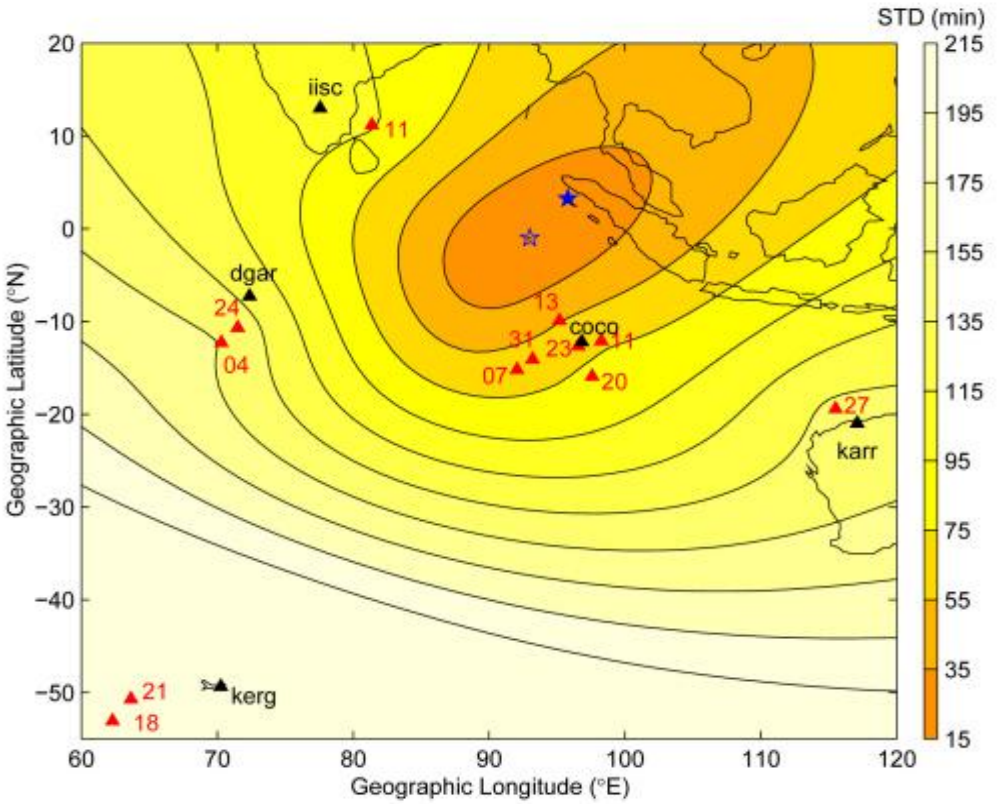


**Figure 3**. Contours of standard deviation of the differences between calculated and observed arrival times are shown. Locations of ground-based GPS receivers and associated monitoring stations are denoted by black triangles with station names and red triangles with GPS satellite numbers. Epicenter reported by U.S. Geological Survey and solid and open blue stars denote calculated source, respectively (Liu et al. 2006).

Note that the average horizontal and vertical speeds generally agree with those directly estimated from the time delay (Figure 4). Meanwhile, the estimated tsunami source location and the induced time are close to the epicenter and origin time of the earthquake given by the U.S. Geological Survey (http://earthquake.usgs.gov/eqcenter/eqinthenews/2004/usslav/).

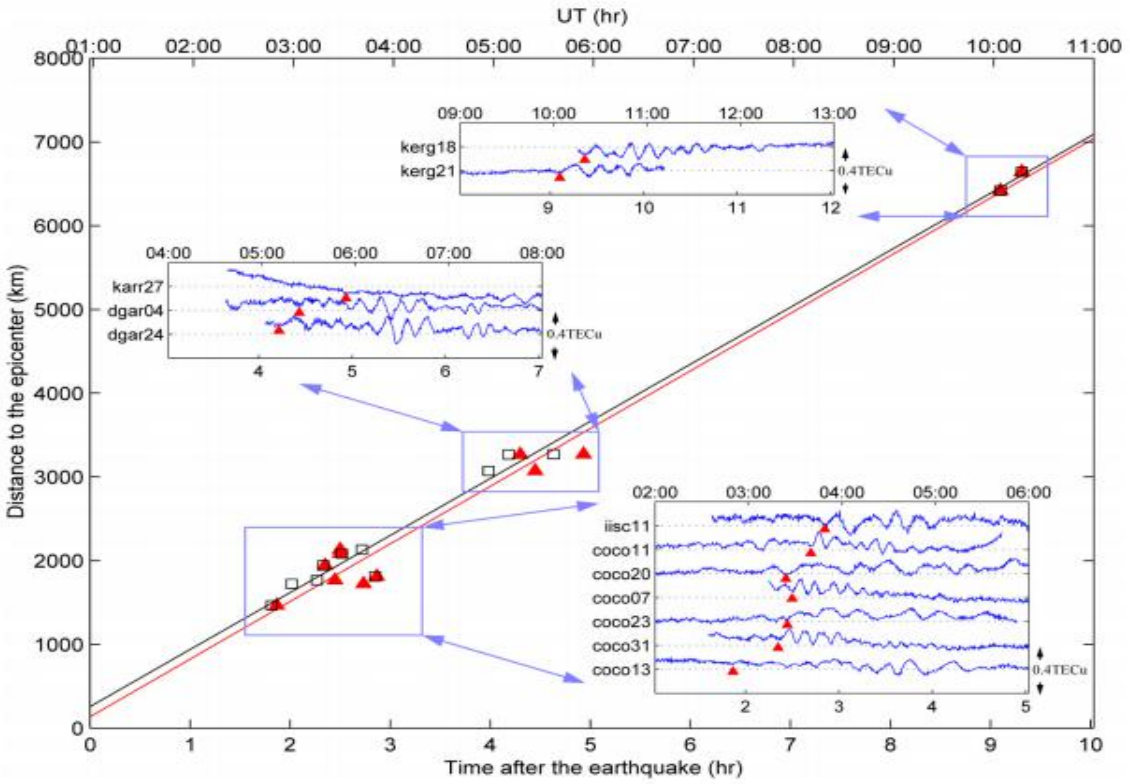


Figure 4. Average horizontal speeds of TIDs and tsunamis are shown. Arrival times (red triangles) vs. distance from epicenter to each monitoring station are employed to compute average horizontal speed of TIDs (red line). Arrival times of tsunami (black squares) at footprints (sub ionospheric points) of monitoring stations, which are extracted from published simulation results, are used to find average horizontal speed of tsunami (black line). Average vertical speed of acoustic gravity waves is estimated from time lag between the two lines (Liu et al. 2006).

### 2.7 Tsunami ionospheric hole (TIH)

A TEC depression with a radius of a few hundred kilometres, which remained stationary for approximately 1 hour was observed (Kakinami et al. 2012). This was termed as the tsunami ionospheric hole (TIH). A TIH was also visible after the Sumatra EQ and the 2010 M8.8 Chile EQ. Further investigations revealed that TIHs appeared after other megathrust and shallow global EQs with magnitudes greater than 7.215 (Astafyeva et al. 2013). A numerical simulation of the TIH elucidated the plasma dynamics. When the acoustic waves

reached the ionosphere, the amplitude of the acoustic waves was intensified due to the very low density of neutral atmosphere. The acoustic waves forced the ionospheric plasma to considerably migrate only along the magnetic field line because of neutral-ion drag. Subsequently, in the decompression phase of the acoustic waves, the downward plasma caused dissociative recombination and suppressed ion production, creating a TEC depression, i.e. TIH. The immediate recombination and slow production caused the TIH to exist for a long time (Shinagawa et al. 2013), According to Astafyeva et al. (2013) reported a correlation not only between initial tsunami height and initial TEC enhancement amplitude, but also between initial tsunami height and TIH duration for 11 large global EQs.

Thus, the quantitative relationship between the initial tsunami height and amplitude of the TEC disturbance immediately above the tsunami source area is required to assess the possibility of using GPS-TEC ionospheric monitoring for a practical early warning system. According to Kamogawa et al.(2016) focus on the value of a TEC depression in a TIH to estimate initial tsunami height, because the TIH remains stationary. They discuss the possibility of constructing an early warning system using only the existing GPS network.

To derive the TEC disturbance caused by the TIH, According to Kamogawa et al.(2016) applied the following procedure. First, the least-squares quadratic curve of the slant TEC time-series in the period from 30 minutes prior to 40 minutes after the main shock was obtained, except for the Tohoku EQ and the Maule EQ. For the Tohoku and Maule EQs, only the period from 30 minutes prior to 7 minutes after the main shock was used because the TIH was too large to obtain appropriate approximation after the TIH. Peculiar bias components for each satellite and the receivers were reduced by the difference between this fitting curve and the raw data. Second, the difference in the vertical TEC (i.e. ΔvTEC) was derived by multiplying the cosine between the slant direction and the satellite earth direction by the difference between the fitting curve and the raw data. The period of the spectrum analysis was 4096 seconds, consisting of 1024-second data of ΔvTEC located in a constant part of a boxcar window function. The vertical axis indicates the distance between the SIP at the time of the main shock and the centre of the tsunami source area, and the horizontal axis indicates the period of the spectrum.

Several resonant modes of acoustic waves occurred; in particular, they were intense in the period from 150 to 210 seconds above the tsunami source area. According to Watada and Kanamori (Watada and Kanamori, 2010), the observed distinct patterns from 150 to 210 seconds are inferred to be resonant modes of the acoustic waves excited by the tsunami. To exclude the variations of resonance modes including the initial TEC pulse, i.e. the acoustic wave components, and extract the component of the TIH, the±150 sec running mean of ΔvTEC except the Niigataken Chuetsu-oki EQ was taken, i.e. low pass filter (LPF) ΔvTEC. For the Niigataken Chuetsu-oki EQ,± 90 sec running means is used because of a small TEC disturbance.

The following procedure was employed to estimate the value of the TEC depression of the TIH above the tsunami source area. First, the tsunami source area was defined to be the average location of the Tohoku EQ (N38.0, E143.4), the Maule EQ (S34.8, W72.9), and the Illapel EQ (S30.9, W72.3) reported by several articles 28–31,26,27,32, and equivalent to the epicentre of other small EQs. Time-series of LPF ΔTEC to estimate the TEC depression

were selected such that the SIP at the time 7 min after the main shock was located within 100 kilometres from the tsunami source area of Mw≥ 8 EQs and 50 kilometres from the epicentre of the other EQs from 7 minutes to 24 (the Tohoku and Maule EQs) and 16 (the other EQs) minutes after the mainshock. They defined δ vTECTIH as the difference between the value of the LPF ΔvTEC 7 minutes after the main shock and the minimum value of LPF ΔvTEC, and δTmin as the interval between the main shock and the minimum time of LPF ΔvTEC.

Considering the simulation of Shinagawa et al.(2013), the TEC depression of TIH was assumed to be proportional to the electron density in the F2 region immediately before the TEC disturbance, because the depressed plasma migrates downward from the F2 region. In this study, the percentage TEC depression with respect to absolute vTEC, i.e. δvTECTIH/vTEC× 100, was discussed for comparison with different solar conditions such as during different seasons and at different local times. For derivation of absolute vTEC, data of Global Ionosphere Maps Total Electron Content (GIMTEC: ftp://ftp.unibe.ch/aiub/CODE/) was used. Finally, the average values and standard deviations of the percentage TEC depression (δvTECTIH/vTEC× 100) and δTmin for each EQ from the selected time-series of LPF ΔvTEC were obtained.

They focused on the percentage TEC depression caused by the TIH and the interval δTmin between the time of the main shock and the minimum value of LPF ΔvTEC (namely the largest TIH). The relationship between the percentage of the TEC depression, δTmin, initial tsunami height and EQ magnitude are illustrated in Fig. 5. As shown in Fig 5a, the percentage of TEC depression versus the initial tsunami height are correlated. In Fig. 5a, the Maule EQ (D) is slightly large, probably because the night-time small background TEC yielded relatively large error of the percentage of TEC depression, while δTmin of the Maule EQ shown in Fig. 5b seems appropriate. On other hand, in Fig. 5c, the four small EQs with small simulated initial tsunami height (A, B, C, and E) seems inappropriate, probably because of difficult identification for the small depression, while the percentage of TEC depression for them are relatively appropriate. Thus, the EQ with more than 1 m initial tsunami height during daytime might show a precise percentage of TEC depression and δTmin.

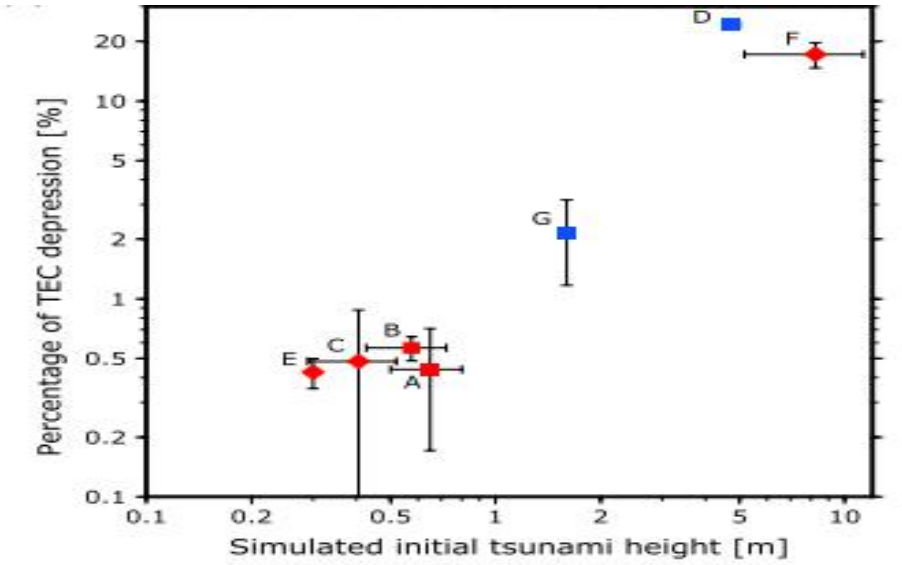


(a)

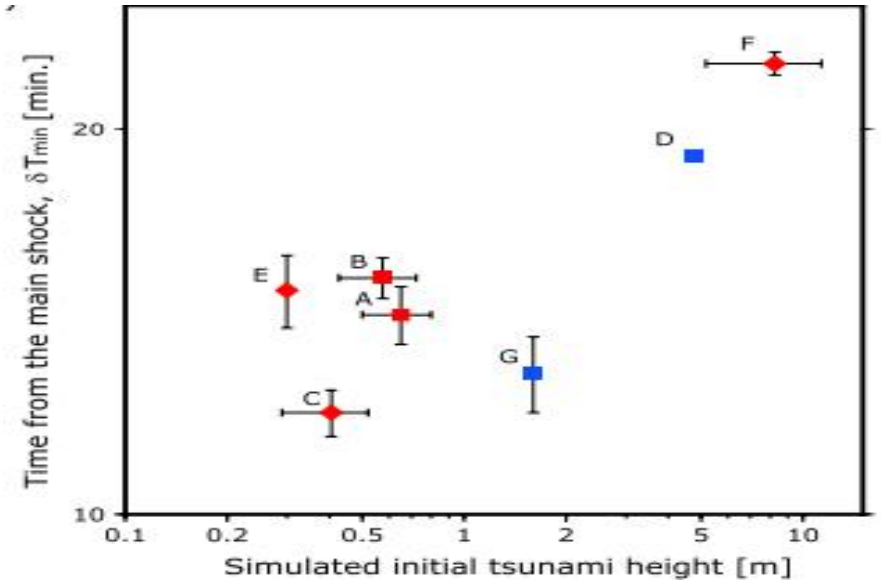


(b)

**Figure 5.** Relationship between percentage TEC depression and initial tsunami height and magnitude. A, B, C, D, E, F and G denote the 2003 M8.0 Tokachi-oki EQ and the 2004, M7.4 Off the Kii peninsula EQ, the 2007 M6.6 Niigataken Chuetsu-oki EQ, the 2010 M8.8 Maule EQ, the 2011 M7.0 Sanriku EQ, the 2011 M9.0 Tohoku EQ, and the 2015 M8.3 Illapel EQ. Red and blue means EQ in Japan and Chile, respectively. Rhombus and squares mean daytime (6–18 LT) and nighttime EQs in local time. (a) Initial tsunami height versus percentage TEC depression. (b) Initial tsunami height versus time after main shock (ΔTmin) (Kamogawa et al. 2016).

## 3. APPLICATION OF GNSS NETWORKS IN INDONESIA FOR TSUNAMI EARLY WARNING SYSTEM AUGMENTATION

### 3.1 Real Time GNSS Data In Indonesia

Positioning system in Indonesia which is carried out systematically and Continuity began in 1989. In that year activities began to take place Global Positioning System for Geodynamic Projects in Sumatra (GPS-GPS) to monitor active tectonic plate motion in Sumatra faults (C. Subarya, 2010). In 1991, The research project collaboration between BAKOSURTANAL and Scripps Institution of Oceanography and Rensselaer Polytechnique Institute, New York, United States of America was expanded to Eastern Indonesia to monitor active tectonic plate movements on "Triple Junction Plate". In 1992, along with the implementation of measurements GPS for the purposes of geodynamic research, GPS measurements are made for procurement Homogeneous and continuous National Horizontal Geodesy Control Network (JKHN) geometrically, and classified as Zero Order JKHN. Next year which is the same and the following year (up to 1994 status) a network expansion was made to lower order, and classified as Order One JKHN. In 1996 s.d 1998 The geodetic control net continues to be developed covering South Asia and Asia Southeast as part of the Geodynamic of South and Southeast Asia Project program (GEODYSSEA) which is a collaboration between BAKOSURTANAL and related agencies inside country and involve earth science researchers from the European Union (C. Subarya, 2010). Then since the early 2000s effectively began implemented continuous GPS (cGPS) observations (C. Subarya, 2010) which is the forerunner to InaCORS. The Aceh tsunami on December 26, 2004 contributed to the increase the number of cGPS stations in Indonesia. Counted several cGPS stations were built at the time in line with the German-Indonesia Tsunami Early Warning System (GITEWS) program. BAKOSURTANAL itself, in 2010 carried out massive cGPS development in tandem with the Indonesia Tsunami Early Warning System (InaTEWS) program. Counted number 40 cGPS stations were built on Java and began to be equipped with data communication systems in the form of a Virtual Private Network (VPN) so that cGPS stations can streaming data in the form of Radio Technical Commission for Maritime Services (RTCM) format to the GPS data center in the Cibinong BAKOSURTANAL office. In the BAKOSURTANAL GPS data center is installed the Networked Transport of software RTCM via Internet Protocol (NTRIP) Caster. The cGPS station besides functioning to monitor the movement of the related tectonic plates for the purposes of InaTEWS has also been able provide position correction services to RTK users. On the basis of the 2011 Geospatial Informaion Law, BAKOSURTANAL has changed its name to Geospatial Information Agency (BIG) which has full authority related to the administration of geospatial information in Indonesia. In 2013 the InaCORS network was utilized in the operation of the Indonesian Geospatial Referens System (SRGI 2013). Starting in 2013, InCORS is growing rapidly, so up to 2019 has been built 207 InaCORS stations spread across all regions of Indonesia as depicted in Figure 7.

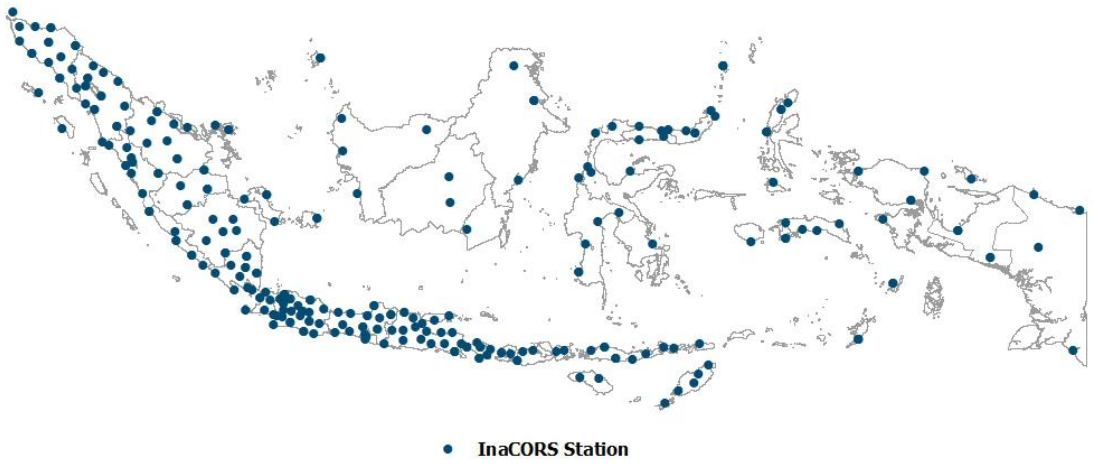


Figure 7. Distribution of InaCORS stations in Indonesia on April 2020

### 3.2 Methodology of INATEWS Augmentation using real time GNSS

Based on reviews of methodology for tsunami detection using ionospheric TEC, we plan to develop a methodology for INATEWS augmentation as shown in Figure 6. As illustrated in Figure 6, GNSS based INATEWS augmentation methodology are as follows. Firstly, the accessing and processing real-time RTCM GNSS data . Using the decoderrtcm.m function, GNSS data RTCM format is converted to ASCII data in PC memory. GNSS observation data was taken from RTCM data are pseudorange on L1 frequency (P1), pseudorange on L2 frequency (P2) , number of phases of carrier wave (number of cycles) on L1 frequency (L1), number of cycles on L2 frequency (L2), satellite number, epoch and position of GNSS station. Secondly the GNSS stastin position data and GPS satellite orbit data are used for calculation of ionospheric pierce point (IPP) coordinate and elevation. IPP elevation data can be used for the conversion of Slant TEC (STEC) to vertical TEC (VTEC). The VTEC data from the carrier phase data are still contain receiver bias, satellite bias, and unknown integer ambiguity cycles (N). Therefore all biases of VTEC are eliminated by using detrending method such as by subtracting VTEC at epoch t (VTEC(t)) with VTEC data on previous epoch (VTEC t-1) to obtain detrended VTEC (DVTEC). DVTEC needs to be filtered to identify the ionospheric accoustic - gravity wave caused by the tsunami by using a bandpass filter in the frequency range with a period of 3 - 33 minutes. DVTEC is filtered from the effects of acoustic-gravity waves to obtain LPF DVTEC to find the tsunami ionospheric hole (TIH) parameter, the decrease percentage in TEC due to the acoustic wave generated by the tsunami. Finally the tsunami parameters can be derived from ionosphere: the initial height of the tsunami from the TIH, the tsunami periode from the DVTECF data, and the tsunami velocity from the delay of ionosphere gravity-acoustic wave observed by single receiver from different GNSS satellites.

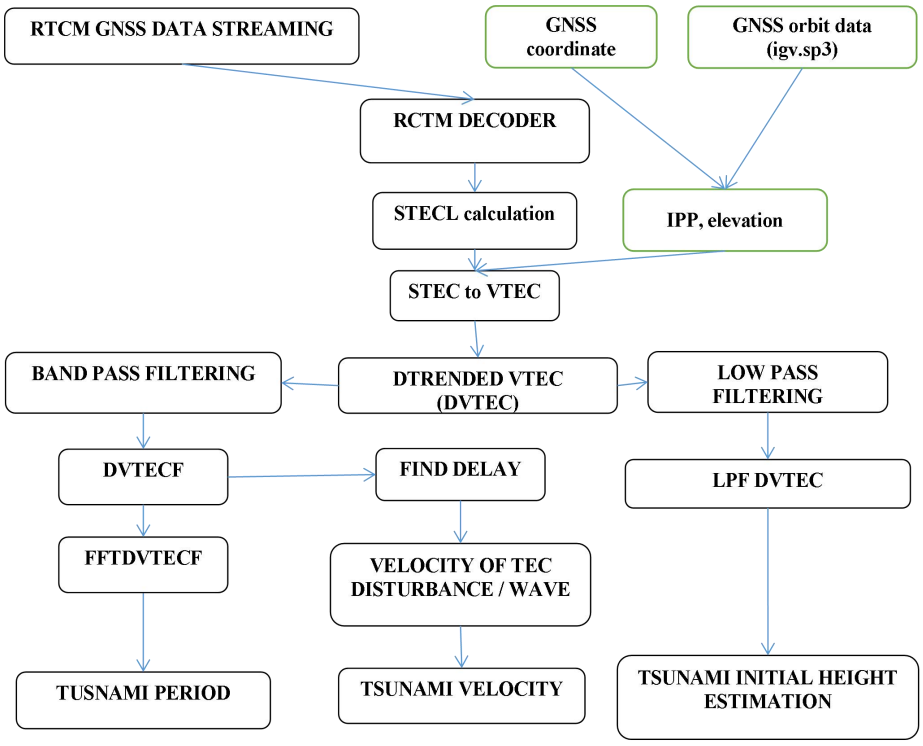


***Fig. 6.*** Methodology for INATEWS augmentation

### 3.3 Real Time MSTID Monitoring Using Single GNSS Station

From one GNSS station, TEC spectrum analysis can be developed in real time by averaging detrended TEC every minute. After collecting the TEC detrended data every minute in 30 minutes, a spectrum analysis is updated every minute. Figure 8 showed the TEC spectrum from Tangerang station.

Figure 8 showed the DSTEC data for 30 minutes of observation derived from the average DSTEC every second. DSTEC spectral analysis for 30 minutes at a certain minute is illustrated by the DSTEC spectral contour of the middle panel of Figure 8. The abscissa of the middle panel of Figure 8 is GPS time, and it's ordinate is the DSTEC fluctuation period in minutes. The right panel of Figure 8 is the location of the ionospheric observation point (IPP) of the CTGR GNSS station in Tangerang on April 18, 2018.

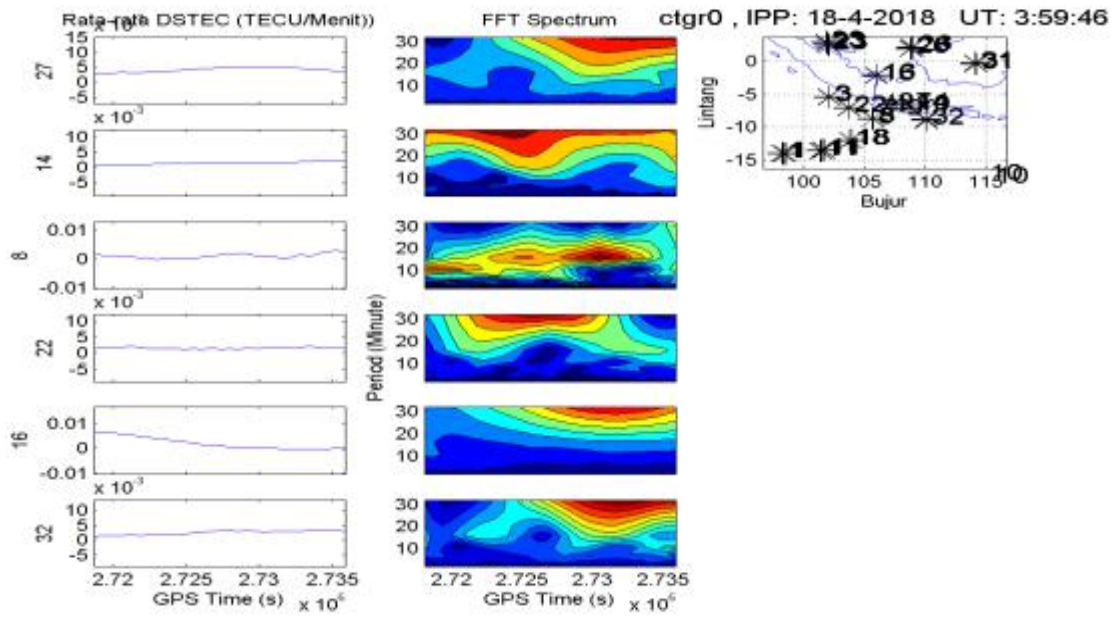


Figure 8. TEC spectrum from Tangerang station

## 4.CONCLUSIONS AND RECOMMENDATION

Since the Aceh Tsunami of December 26, 2004 and Tohoku tsunami of March 11, 2011, researchers have proven that TEC data from GNSS phase data can be utilized for the detection of tsunami effects on the ionosphere and can be used for estimating the tsunami epicenter, direction and speed, with the same method of epicenter determination from seismic data. Beside the ionospheric wave, tsunami ionospheric holes have been found and they have a relationship with the initial high of tsunami. Tsunami effect on the ionosphere can be detected by using filtering methods such as high pass filtering, band pass filtering, polynomial filtering, and TEC difference. The researchers believe that TEC GNSS can be used to strengthen existing tsunami early warning systems. But until now the detection of tsunami effects on the ionosphere is still in the research stage with off-line GNSS data. The implementation of tsunami detection using GNSS TEC requires real time GNSS data access in RTCM format.Tsunami effect detection methods with real time GNSS data that can be used for InaTEWS augmentation needs to be modified to estimate the tsunami effect on the ionosphere, determining the speed and direction of tsunami propagation in real time with a delay of several minutes. Unfortunately, the augmentation of TEWS with GNSS TEC data is only effective for large tsunamis and the epicenter is located 200 km farther from the coast. The InaTEWS augmentation by using real time GNSS TEC is under development and currently in the real time multi-station TEC estimation stage and TEC real time analysis spectrum from single GNSS station.

Acknowledgment

This research was funded through the INSINAS program of the Indonesian Ministry of research technology and higher education (No. 14/INS/PPK/E4/2020). And we gratefully thank the Indonesian Geospatial information agency for support in the preparation GNSS real time data. Also, Well deserved recognition is due to Joni Efendi for his consultations and suggestions for using GNSS RTCM data for real time TEC purposes.

## REFERENCES

Aki K and Richards P (2002), Quantitative Seismology, University Science Books (Sausalito).

Artru J, Ducic V, Kanamori H, Lognonné P and Murakami M (2005), Ionospheric detection of gravity waves induced by tsunamis, Geophys. J. Int, 160 840-48.

Astafyeva E, Shalimov S, Olshanskaya E and Lognonné P (2013), Ionospheric response to earthquakes of different magnitudes: Larger quakes perturb the ionosphere stronger and longer, Geophys. Res. Lett, 40 1675-81.

Babeyko A and Hoechner A (2012), Accuracy of tsunami source inversion with real-time GPS, Geophysical Research Abstracts, Deutsches GeoForschungsZentrum, Potsdam, Germany, Vol 14 EGU2012-4571.

Balasis G. and Mandea M.(2007), Can electromagnetic disturbances related to the recent great earthquakes be detected by satellite magnetometers?, special issue Mechanical and Electromagnetic Phenomena Accompanying Preseismic Deformation: from Laboratory to Geophysical Scale, ed. by K. Eftaxias, T. Chelidze and V. Sgrigna, Tectonophysics,431, doi:10.1016/j.tecto.2006.05.038

DasGupta A, Das A, Hui D, Bandyopadhyay K and Sivaraman M (2006), Ionospheric perturbation observed by the GPS following the December 26th, 2004 Sumatra-Andaman earthquake, Earth Planet Sp, 58 167-72.

Galvan D, Komjathy A, Hickey M and Mannucci A (2011), The 2009 Samoa and 2010 Chile tsunamis as observed in the ionosphere using GPS total electron content, J. Geophys. Res, 116 A06318.

Ge M, Dousa J, Li X, Ramatschi M, Wickert J (2011), Development of the GFZ real-time precise point positioning service, Geophysical Research Abstracts, Vienna, Austria, Vol 13 EGU2011-3865.

Hanka W, Saul J, Weber B, Becker J, Harjadi P, Fauzi and et al (2010), Real-time earthquake monitoring for tsunami warning in the Indian Ocean and beyond, Nat. Hazards Earth Syst. Sci. European Geosciences Union, Vol 10 2611-2622 22.

Hickey M, Schubert G and Walterscheid R (2009), Atmospheric airglow fluctuations due to a tsunami-driven gravity wave disturbance, J. Geophys. Res, 115 A06308.

Hines C (1972), Gravity waves in the atmosphere, a nature research journal, 239 73-78.

Hines C (1974), The upper atmosphere in motion, Geophysical Monograph Series, Washington, D.C, vol 18.

Iyemori T, Nose M, Han D, Gao Y, Hashizume M, Choosakul N, and et al (2005), Geomagnetic pulsations caused by the Sumatra earthquake on December 26, 2004, Geophys. Res. Lett, 32 L20807.

Jin S, Occhipinti G and Jin R (2009), GNSS ionospheric seismology: recent observation evidences and characteristics, Earth-Science Reviews, 147 54-64.

Jin S, Jin R and Li J (2014), Pattern and evolution of seismo-ionospheric disturbances following the 2011 Tohoku earthquakes from GPS observations, J. Geophys. Res. Space Physics, 119 7914-27.

Kakinami Y, Kamogawa M, Tanioka Y, Watanabe S, Gusman A, Liu J, and et al (2012), Tsunamigenic ionospheric hole, Geophys. Res. Let, 39 L00G27.

Kamogawa M, Orihara Y, Tsurudome C, Tomida Y, Kanaya T, Ikeda D, and et al (2016), A possible space-based tsunami early warning system using observations of the tsunami ionospheric hole, Sci. Rep, 6 37989.

Lay T, Kanamori H, Ammon C, Nettles M, Ward S, Aster R, et al (2005), The great Sumatra-Andaman earthquake of 26 December 2004, Science, 308 1127-32.

Le Pichon A, Herry P, Mialle P, Vergoz J, Brachet N, Garces M, and et al (2005), Infrasound associated with 2004–2005 large Sumatra earthquakes and tsunami, Geophys. Res. Lett, 32 L19802.

Liu J, Lin C, Chen Y, Lin Y, Fang T and Chen C (2006), Solar flare signatures of the ionospheric GPS total electron content, J. Geophys. Res, 111 A05308.

Liu J, Tsai Y, Ma K, Chen Y, Tsai H, Lin C, et al (2006), Ionospheric GPS total electron content (TEC) disturbances triggered by the 26 December 2004 Indian Ocean tsunami, J. Geophys. Res, 111 A05303. Vol 39 No. 2, page 84 (2020)

Lognonné P, Artru J, Garcia R, Crespon F, Ducic V, Jeansou E, et al (2006), Ground-based GPS imaging of ionospheric post-seismic signal, Planet. Space Sci, 54 (5) 528-40.

Mai C and Kiang J (2009), Modeling of ionospheric perturbation by 2004 Sumatra tsunami, Radio Sci, 44 RS3011.

Matsumura M, Saito A, Iyemori T, Shinagawa H, Tsugawa T, Otsuka Y, and et al (2014), Numerical simulations of atmospheric waves excited by the 2011 off the Pacific coast of Tohoku Earthquake, Earth, Planets and Space, 63 885-89.

Occhipinti G, Lognonné P, Kherani A and Hébert H (2006), Three-dimensional waveform modeling of ionospheric signature induced by the 2004 Sumatra tsunami, Geophys. Res. Lett, 33 L20104.

Occhipinti G, Lognonné P, Kherani A and Hébert H (2006), The indian ocean tsunami 2004 in the ionosphere : observations and modelling AGU fall meeting San Francisco.

Occhipinti G, Alam Kherani E, Lognonné P (2008), Geomagnetic dependence of ionospheric disturbances induced by tsunamigenic internal gravity waves, Geophys. J. Int, 173 (3) 753-65.

Occhipinti G, Rolland L, Lognonné P and Watada S (2013), From Sumatra 2004 to Tohoku-Oki 2011: The systematic GPS detection of the ionospheric signature induced by tsunamigenic earthquakes, J. Geophys. Res. Space Physics, 118 3626-36.

Park J, Song T, Tromp J, Okal E, Stein S, Roult G, et al (2005), Earth's free oscillations excited by the 26 December 2004 Sumatra-Andaman earthquake, Science 308 1139-44.

Peltier W and Hines C (1976), On the possible detection of tsunamis by a monitoring of the ionosphere, J. Geophys. Res, 81 1995-2000.

Shinagawa, H., T. Tsugawa, M. Matsumura, T. Iyemori, A. Saito, T. Maruyama, and et al (2013), Two-dimensional simulation of ionospheric variations in the vicinity of the epicenter of the Tohoku-oki earthquake on 11 March 2011, Geophys. Res. Lett, 40 5009-13.

Smith, W., R. Scharroo, V. Titov, D. Arcas, and B. Arbic (2005), Satellite altimeters measure tsunami, Oceanography, Vol 18, No. 2.

Subarya C (2004), The Maintenance of Indonesia Geodetic Control Network - In the Earth Deforming Zones, Paper of the 3rd FIG Regional Conference.

Subarya, C. 2010. Modeling and Estimation of the Dynamics of Tectonic Plate Movement in Indonesian Territory from GPS Observation. Dissertation. ITB Post-graduate Program. Bandung..

Tsugawa T, Saito A, Otsuka Y, Nishioka M, Maruyama T, Kato H, and et al (2011), Ionospheric disturbances detected by GPS total electron content observation after the 2011 off the Pacific coast of Tohoku Earthquake, Earth, Planets and Space, 63 875-79.

Vigny C, Simons W, Abu S, Bamphenyu R, Satirapod C, Choosakul N, and et al (2005), Insight into the 2004 Sumatra-Andaman earthquake from GPS measurements in southeast Asia, Nature, 436 201-06.

Watada S and Kanamori H (2010), Acoustic resonant oscillations between the atmosphere and the solid earth during the 1991 Mt. Pinatubo eruption, J. Geophys. Res, 115 B12319.

Wei Y, Titov V, Newman A, Hayes G, Liujuan T and Chamberlin C (2011), Near-field hazard assessment of March 11, 2011 Japan tsunami sources inferred from different methods, OCEANS 2011, IEEE Conference Publications, 1–9